J. Membrane Biol. 169, 199–207 (1999)

The Journal of
Membrane
Biology

Distortion Component Analysis of Outer Hair Cell Motility-Related Gating Charge

S. Takahashi, J. Santos-Sacchi
Sections of Otolaryngology and Neurobiology, Yale University School of Medicine, New Haven, CT 06510, USA

Received: 31 December 1998/Revised: 12 March 1999

Abstract. The underlying Boltzmann characteristics of motility-related gating currents of the outer hair cell (OHC) are predicted to generate distortion components in response to sinusoidal transmembrane voltages. We studied this distortion since it reflects the mechanical activity of the cell that may contribute to peripheral auditory system distortion. Distortion components in the OHC electrical response were analyzed using the whole-cell voltage clamp technique, under conditions where ionic conductances were blocked. Single or double-sinusoidal transmembrane voltage stimulation was delivered at various holding voltages, and distortion components of the current responses were detected by Fourier analysis. Current response magnitude and phase of each distortion component as a function of membrane potential were compared with characteristics of the voltage-dependent capacitance, obtained by voltage stair-step transient analysis or dual-frequency admittance analysis. The sum distortion was most prominent among the distortion components at all holding voltages. Notches in the sum (f1+f2), difference (f2−f1) and second harmonic (2f) components occur at the voltage where peak voltage-dependent capacitance resides (V_{pkCm}). Rapid phase reversals also occurred at V_{pkCm}, but phase remained fairly stable at more depolarized and hyperpolarized potentials. Thus, it is possible to extract Boltzmann parameters of the motility-related charge movement from these distortion components. In fact, we have developed a technique to follow changes in the voltage dependence of OHC motility and charge movement by tracking the voltage at phase reversal of the f2−f1 product. When intracellular turgor pressure was changed, V_{pkCm} and distortion notch voltages shifted in the same direction. These data have important implications for understanding cochlear nonlinearity, and more generally, indicate the usefulness of distortion analysis to study displacement currents.

Key Words: Outer hair cell — Distortion — Gating charge — Membrane capacitance — Turgor pressure

Introduction

In linear systems, input and output signals contain the same in-phase frequency components. In nonlinear systems, stimulus frequencies (single: f1; two-tone; f1, f2) produce harmonic and combination distortion components, such as nf1, (n+1)f1−nf2 and (n+1)f2−nf1 (n = 1,2,3, . . .). Distortion is readily perceived by the auditory system despite the purity of acoustic stimuli (Goldstein, 1967). Physiological correlates of the perceived distortion exist in responses of auditory nerve fibers (Goldstein & Kiang, 1968; Kim, Molinar & Matthews, 1980), inner hair cells (Nuttall & Dolan, 1990), and basilar membrane vibration patterns (Robles, Ruggero & Rich, 1991, 1997). Such distortion, which is dependent upon normal outer hair cell (OHC) function, clearly reveals the nonlinear nature of peripheral auditory processing. OHCs are the primary source of distortion components in mammals.

The OHC produces voltage-dependent mechanical responses that provide feedback into the basilar membrane, thereby sharpening the passive mechanical vibration of the cochlear partition (Brownell et al., 1985; Ashmore, 1987; Santos-Sacchi & Dilger, 1988; Ruggero, 1992). The cell also possesses a nonlinear gating charge movement or correspondingly, a voltage-dependent capacitance, which correlates well with its mechanical activity (Ashmore, 1989; Santos-Sacchi, 1990, 1991). The underlying nonlinear Boltzmann characteristics of the charge movement and mechanical response are predicted to generate distortion components in the response to single and dual sinusoidal transmembrane volt-

Correspondence to: J. Santos-Sacchi

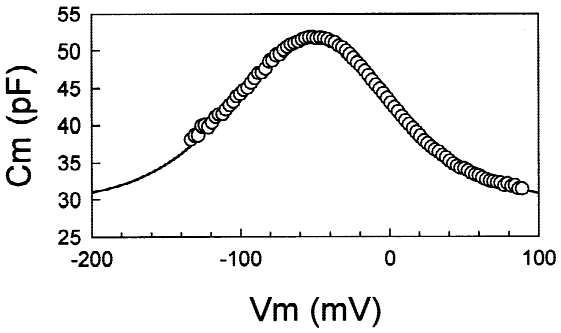

Fig. 1. Outer hair cell voltage-dependent capacitance determined from FFT-based dual-sinusoidal technique (Santos-Sacchi et al., 1998). Fit to Eq. 1 indicates V_{pkCm}: −52.6 mV; z: 0.71; Q_{max}: 3.22 pC; and C_{lin}: 29.6 pF.

ages. Indeed, OHCs generate mechanical distortions when stimulated under voltage clamp (Santos-Sacchi, 1993) or transcellularly within a pipette microchamber (Hu et al., 1994). The purpose of the present experiments is to describe the features of OHC electrical distortion components that arise from motility-related charge movement. These electrical distortion components reflect the mechanical activity of the OHC and thus are useful in understanding the generation of mechanical distortion that is present in the peripheral auditory system. While the data have important implications for understanding cochlear nonlinearity, more generally, they illustrate the type of behavior expected from nonlinear membrane charge movement regardless of source (e.g., from ionic channels).

A preliminary presentation of these data has been made (Takahashi & Santos-Sacchi, 1997).

Materials and Methods

General

OHCs and supporting cells were freshly isolated from the organ of Corti of the guinea-pig cochlea and transferred to a 700 μl perfusion chamber (Kakehata et al., 1995) filled with an external standard solution. The external standard solution contained (in mM): 142 NaCl, 5.37 KCl, 1.25 $CaCl_2$, 1.48 $MgCl_2$, 10 HEPES and 5 dextrose, pH 7.2, 300 mOsm. OHCs were whole-cell voltage clamped using an Axon 200B amplifier with patch pipettes having initial resistances of 2–3 MΩ. Residual series resistance ranged from 3–7 MΩ. To remove voltage-dependent ionic conductances, the external standard solution was replaced with an ionic blocking solution during electrical recording. The external ionic blocking solution contained (in mM): 100 NaCl, 20 TEA, 20 CsCl, 2 $CoCl_2$, 1.52 $MgCl_2$, 10 HEPES and 5 dextrose, pH 7.2, 300 mOsm (adjusted with dextrose). The patch pipette solution contained (in mM): 140 CsCl, 2 $MgCl_2$, 10 EGTA and 10 HEPES, with pH 7.2 and osmolarity 300 mOsm (adjusted with dextrose). Thus, capacitive currents could be analyzed in isolation (Santos-Sacchi, 1991; Huang & Santos-Sacchi, 1993; Kakehata & Santos-Sacchi, 1995). Salicylate (10 mM) or lutetium chloride (3 mM) was used to reduce motility related gating charge movement in some experiments (Kakehata & Santos-Sacchi, 1996).

Pipette pressure was modified with a syringe connected to the Teflon tubing attached to the patch pipette holder. Pressure was monitored via a T-connector to a pressure monitor (WPI, Sarasota, FL). δz, longitudinal strain, a unit-less metric, was calculated as $\Delta L/L_0$, where ΔL is the change of cell length due to turgor pressure change and L_O is the original cell length. All experiments were performed at room temperature (~23°C).

Evaluation of Membrane Capacitance

Detailed evaluation of membrane capacitance was made at different potentials by transient analysis of currents induced by a voltage stair step stimulus (−150 to +50 mV, 10 mV increments; Huang & Santos-Sacchi, 1993), or by FFT-based admittance analysis of dual voltage sinusoidal stimulation (Santos-Sacchi et al., 1998); the capacitance data were fit to the first derivative of a two state Boltzmann function relating nonlinear charge to membrane voltage (Santos-Sacchi, 1991),

$$C_m = C_v + C_{lin} = Q_{max}\frac{ze}{kT}\frac{b}{(1+b)^2} + C_{lin} \qquad \text{Eq (1)}$$

where

$$b = \exp\left(\frac{-ze(V_m - V_{pkCm})}{kT}\right)$$

Q_{max} is the maximum nonlinear charge moved, V_{pkCm} is voltage at peak capacitance or equivalently, at half maximal nonlinear charge transfer, V_m is membrane potential, z is valence, C_{lin} is linear membrane capacitance, e is electron charge, k is Boltzmann's constant, and T is absolute temperature. Series resistance, R_s was estimated from the decaying time constant and integrated charge of the voltage step-induced current, as fully described elsewhere (Huang & Santos-Sacchi, 1993). Membrane resistance, R_m, was evaluated from steady state current. C_{lin} was estimated from the fit to above capacitance (C_m) equation, and indicates the intrinsic linear capacitance of the membrane upon which rides the bell-shaped voltage-dependent capacitance (C_v).

Distortion Measurement

To evoke distortion components, single or two summed sinusoidal membrane voltages were delivered to OHCs under whole-cell voltage clamp at various holding potentials. Peak amplitude of input stimuli was set between 5 and 26 mV. Input stimulus frequencies and frequency ratios (f2/f1) were also varied. The AC stimulus duration was fixed at 51.2 msec, with the sampling at 10 μsec. Data were filtered at 5 kHz (4-pole Bessel). Steady-state current responses were analyzed by Fast Fourier Transform (FFT) to extract the magnitude and phase of distortion components at 2f1 ± f2, 2f2 ± f1, f2 ± f1, 2f1, and 3f1. All data collection and analysis were performed with an in-house developed Window's based whole-cell voltage clamp program, jClamp (www.med.yale.edu/surgery/otolar/santos/jclamp.html), utilizing a Digidata 1200 board (Axon, CA).

Results

After blocking nonlinear conductances in the OHC, the predominant electrical nonlinearity that remains is a voltage-dependent capacitance, which derives from motility-

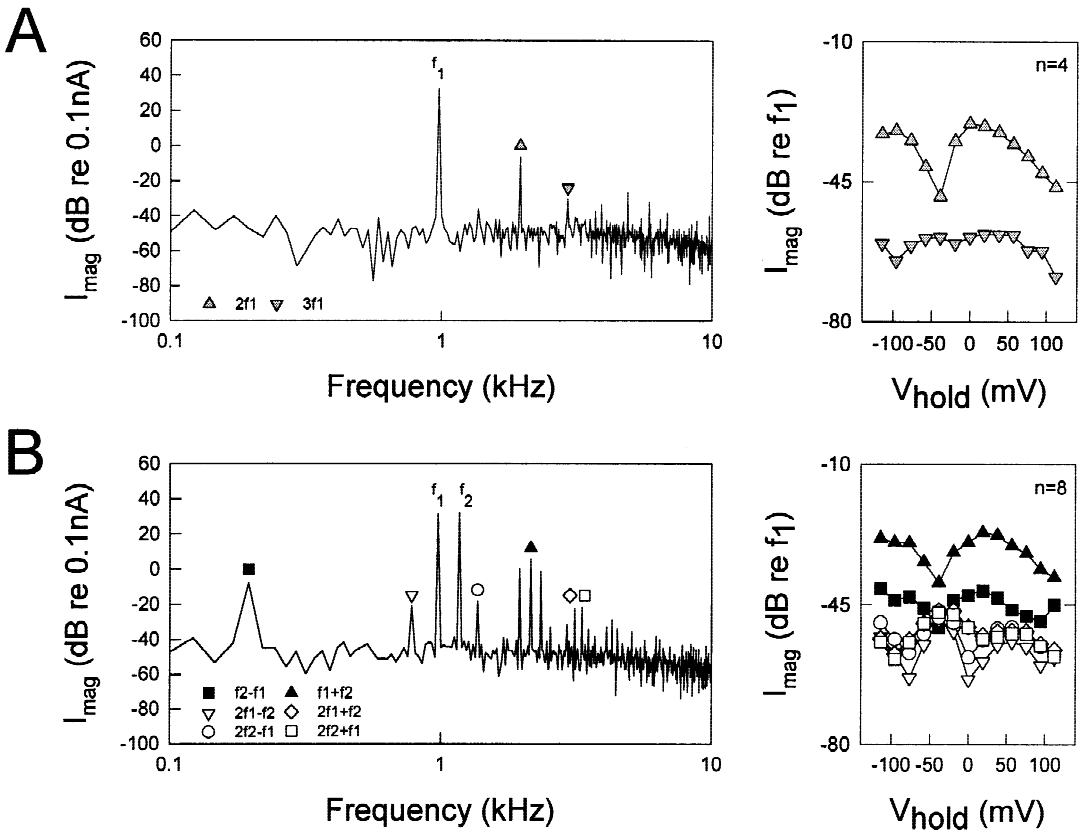

Fig. 2. *Left panels:* Typical frequency spectra of OHC current responses to AC transmembrane voltage stimuli measured under whole cell voltage clamp. Spectra were obtained by fast Fourier transform. Input stimulus frequencies were set at 963Hz (f1) and 1156Hz (f2); magnitudes were 25 mV peak. Induced currents contained (*A*) harmonic distortion components (2f1, 3f1) and (*B*) combination distortion components (f2−f1, f1+f2, 2f1−f2, 2f2−f1), as well as peaks at the primary frequencies. The *right panels* illustrate the average effects of holding voltage (−120 to 120 mV, in 20 mV increments) on distortion component magnitudes (dB re: magnitude at f1). Averaged series and membrane resistances were 4.0 and 259 MΩ, respectively.

related nonlinear charge movement (Fig. 1). Due to this nonlinearity, delivery of single or dual sinusoidal voltages across the OHC membrane elicits current responses that contain the original frequency components as well as distortion components. Fig. 2 (*left panels A* and *B*) shows typical spectra obtained by FFT analysis of current responses evoked by 25 mV AC transmembrane voltage stimuli (f1: 963 Hz and f2: 1156 Hz). In addition to the peaks at the input stimulus frequencies (f1, f2), quadratic distortions (f2±f1), cubic distortions (2f1±f2, 2f2±f1), and second and third harmonic distortions (2f1, 3f1) were detected above the noise floor. The noise floor associated with our measuring system averaged approximately −46.7 dB re 0.1 nA in the 5 kHz bandwidth. Second harmonic, sum (f1+f2) and difference (f2−f1) distortion components were largest. For example, the largest sum component averaged 27 dB down from f1 response magnitude. The *right panels* in Fig. 2 show averaged magnitude responses as a function of holding potential. Second harmonic, sum and difference distortion components exhibit magnitude notches near −40 mV, whereas notches in the other distortion component magnitudes appear at voltages above and below that voltage.

Distortion in cochlear supporting cells, e.g., Deiters cells, which lack the voltage-dependent capacitance characteristic of OHCs, was close to the noise floor (Fig. 3), supporting the view that the extensive distortion arising within the OHC is related to its lateral membrane sensor-motors. Indeed, the voltage dependence of distortion components derives from the Boltzmann characteristics of the robust OHC motility-related nonlinear charge movement and is evident in the representative data ($n = 10$) of Fig. 4 where voltage-dependent capacitance is plotted along with distortion component magnitude and phase. The voltage where magnitude minima are observed in second harmonic, sum and difference components corresponds to the voltage at peak capacitance (V_{pkcm}). Associated with the magnitude minima are abrupt phase reversals. The other distortion component minima are also associated with abrupt phase reversals. Changes in stimulus frequencies (f2: 0.6–1.4 kHz)

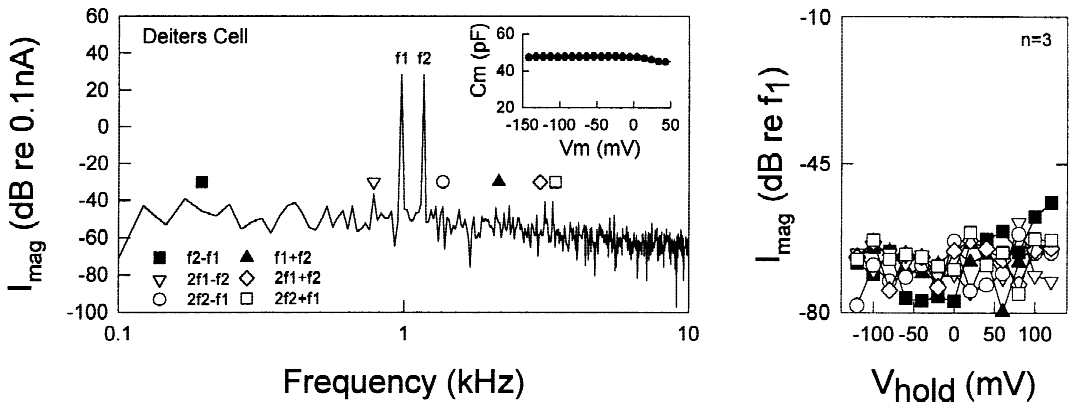

Fig. 3. Distortion components generated in a Deiters supporting cell obtained as in Fig. 2. *Left panel* shows distortion components close to the noise floor. Inset illustrates the linear capacitance of the cell. The *right panel* shows the effect of holding potential. It is clear that supporting cells do not present the degree of nonlinearity that characterizes the OHC.

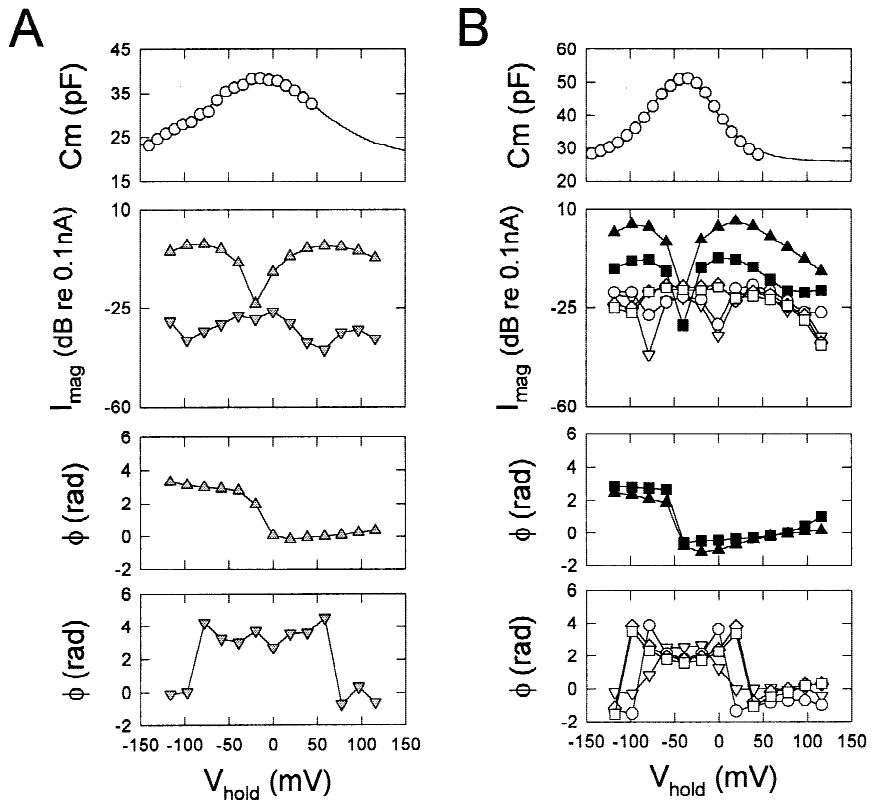

Fig. 4. Relationship between nonlinear capacitance and distortion component magnitude and phase. (*A*) OHC capacitance was determined by the stair step technique. The solid line indicates a fit of this cell's capacitance to Eq. 1: V_{pkCm}: −12.0 mV; z: 0.59; Q_{max}: 3.17 pC; and C_{lin}: 20.3 pF. The bottom panels plot the magnitude and phase of the second and third harmonic. Lines are only connections between symbols. Symbols are as in Fig. 2*A*. Note that the minima in magnitudes correspond to abrupt phase reversals. (*B*) The solid line indicates a fit of this cell's capacitance to Eq. 1: V_{pkcm}: −40.6 mV; z: 1.0; Q_{max}: 2.61 pC; and C_{lin}: 26.0 pF. The bottom panels plot the magnitude and phase of the combination distortion components. Symbols are as in Fig. 2*B*. As above, magnitude minima correspond to abrupt phase reversals.

or frequency ratios (f2/f1: 1.1–1.4) did not alter distortion components. Figure 5 shows the intensity functions for the sum and difference components at three holding potentials, −60, 0 and 60 mV. Distortion decreased at a rate greater than stimulus intensity. Other distortion components showed similar decreases, but in the low range of stimulus intensities disappeared into the noise floor.

Further evidence implicating OHC motility-related nonlinear charge movement as the source of distortion is derived from charge blocking experiments. Both lanthanides and salicylate blocked voltage-dependence capacitance and distortion. Figure 6 illustrates the effects of 3 mM lutetium chloride on nonlinear capacitance and distortion products. The drop in capacitance is mirrored by a decrease in all distortion components. In the case of salicylate, the reductions were reversible (*data not shown*). The correspondence between distortion prod-

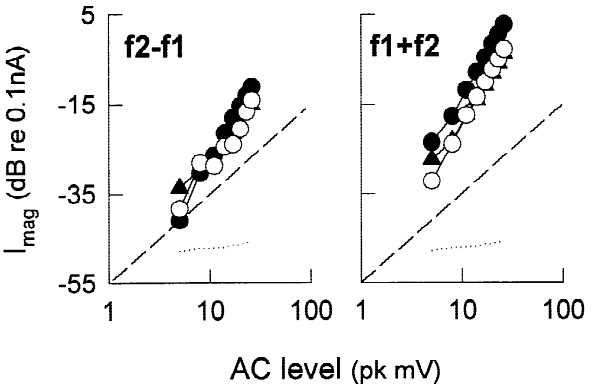

Fig. 5. Sum and difference distortion magnitude as a function of AC stimulus level. Results at three holding potentials are plotted: −60 mV, closed triangles; 0 mV, filled circles; 60 mV, open circles. Both components decrease at a rate greater than the stimulus. The dashed line illustrates a linear relationship. The dotted line is the noise floor.

ucts and nonlinear capacitance can be used to predict alterations in the Boltzmann characteristics. Figure 7 shows the utilization of f2−f1 phase reversal to track peak capacitance and V_{pkcm} during changes in OHC turgor pressure. As intracellular pressure is decreased, indicated by the change in OHC longitudinal strain (δz), C_m increases and V_{pkcm} shifts in the negative direction as observed previously using other techniques (Kakehata & Santos-Sacchi, 1995).

Discussion

The present results indicate that membrane-bound nonlinear charge movement, in this case due to motility voltage sensors residing in the OHC lateral membrane, can lead to distortion component generation under whole cell voltage clamp. Classical studies have used linearized impedance analysis to characterize ionic channel gating charge movement (Fishman, Moore & Ponssart, 1977; Takashima, 1978; Bezanilla et al., 1982; Fernandez, Bezanilla & Taylor, 1982). Indeed, similar analyses have been made on OHC motility-related gating charge (Santos-Sacchi, 1991). However, those studies did not evaluate distortion generation. In the OHC, single frequency voltage stimulation generates harmonic distortion and two-frequency stimulation generates combination distortion in the current responses. The largest components were at the second harmonic (2f), sum (f1+f2) and difference (f2−f1) frequencies, but significant responses were obtained at the more complex combination frequencies. The voltage dependence of the distortion component magnitude and phase derive from the Boltzmann characteristics of the OHC's motility-related gating charge. Thus, it was possible to track changes in V_{pkcm}, or equivalently V_h, the voltage at half-maximal charge

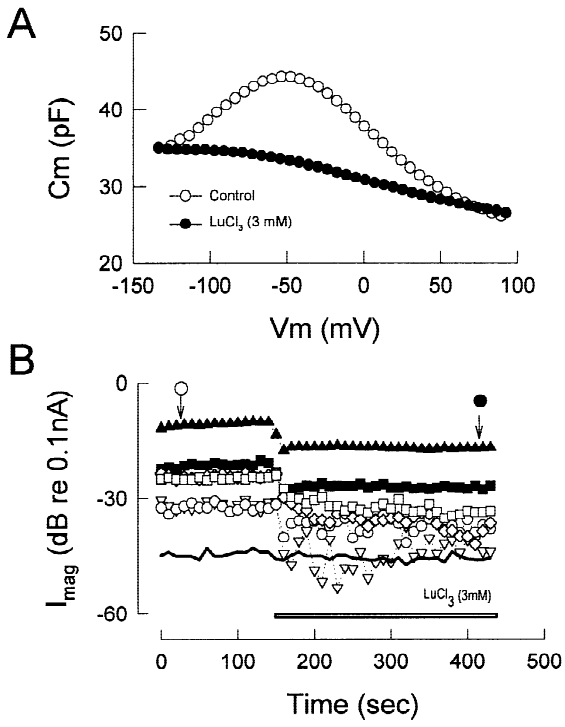

Fig. 6. Effects of charge blocking lutetium chloride on OHC capacitance and distortion. (*A*) Capacitance (measured with dual frequency admittance technique) of OHC before and after 3 mM $LuCl_3$. Fit of control capacitance to Eq. 1 indicates V_{pkcm}: −53.3 mV; z: 0.59; Q_{max}: 3.68 pC; and C_{lin}: 23.4 pF. After treatment the function could not be fit reliably, however, at −60 mV nonlinear capacitance is halved by the treatment. (*B*) After treatment, distortion components measured at a holding potential of −60 mV were down about 6 dB (halved). Symbols are the same as in Fig. 2*B*.

displacement, by monitoring the phase reversal of the f2−f1 distortion component.

The magnitude and phase data are readily predicted from an electrical model of the OHC-patch-clamp system, which includes an electrode resistance in series with a parallel combination of membrane resistance and capacitance, the capacitance being comprised of a linear and voltage-dependent component (*see* Santos-Sacchi, 1993 for details). The voltage-dependent capacitance component is the only nonlinearity in the system. Figure 8 illustrates the response of the model to the same protocols, i.e., single- and two-frequency voltage stimulation, that we used in the experiments on OHCs and supporting cells. The fitted parameters of the two OHCs depicted in Fig. 4 were used in the model to generate the distortion components. The model response compares favorably with the biophysical data (*compare* Figs. 4 and 8), confirming that distortion magnitude minima and phase reversals result from the characteristics of the nonlinear capacitance function, or equivalently, the nonlinear Q-V function. Notably, the nonlinearity in the OHC that we studied is similar to that of ionic channel gating,

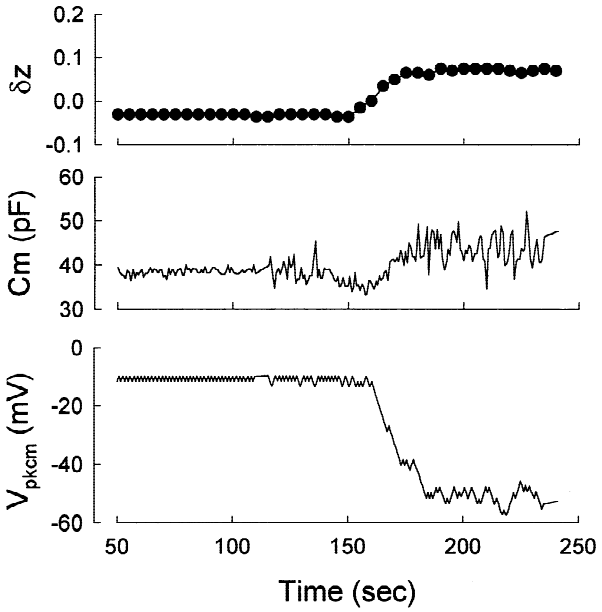

Fig. 7. Utilization of phase data to track changes in Boltzmann characteristics of OHC capacitance. The voltage at which f2−f1 phase reversed (V_{pkcm}) was tracked by altering holding potential in 2 mV increments until a phase reversal occurred, whereupon holding potential was decremented until reversal occurred. The tracking process was continuous while OHC turgor pressure was altered. When turgor pressure was reduced, indicated by an increase in longitudinal strain (δz), C_m increased and V_{pkcm} shifted in the negative direction, in line with previous studies (Kakehata & Santos-Sacchi, 1995).

and therefore it is expected that channel gating will possess a distortion signature that characterizes its voltage-dependent behavior. Indeed, the small distortion components detected in supporting cells may arise from gating of ionic channels. A more selective and detailed analysis directed within an ionic channel's activation voltage range may prove more revealing.

Intermodulation distortion characteristics derived from the form of the mathematical function describing the excited nonlinearity; the magnitudes and phases of distortion are given by the Fourier expansion of the excitation products and are predictable (Dallos, 1973). In the case where a function can be expressed mathematically as a polynomial, AC distortions correspond to the order of the polynomial. Functions of quadratic order produce "quadratic distortions," namely (for dual excitation) f2±f12, and those of cubic order produce "cubic distortions," namely, 2f1±f2, 2f2±f1. Since our data show both types of distortion, it is clear that the two-state Boltzmann function can be characterized by the sum of polynomials with even and odd orders, the relative contribution depending on the holding potential level. Thus, the distortion that we obtained empirically and verified through modeling and experimental perturbation with charge blockers is simply a consequence of the form of an OHC's Q-V function. It should be noted, however, that memory-less characterizations such as this, as in our model, do not take into account the recently observed dependence of the Q-V function on initial voltage conditions (Santos-Sacchi et al., 1998). Thus, the slight differences between model and data may arise from this dependence.

Our data also indicate the need for caution when performing dual sinusoidal capacitance measures (Rohlicek & Rohlicek, 1993; Donnelly, 1994). Because of the large AC voltages typically used with these techniques, it is possible that distortion generated by membrane nonlinearities can interfere with capacitance measures. We used an FFT-based variation of this technique (Santos-Sacchi et al., 1998), but our signal levels were at 10 mV pk, where little distortion was generated in the OHC.

Relevance to the Auditory System

In the mammal, the range of auditory sensitivity spans greater than 100 dB. In order to process this immense range, the system response (e.g., basilar membrane amplitude) grows nonlinearly with stimulus level. As a result, distortion is generated and is the hallmark of the normal auditory system response; it is indicative of an active process that enhances the mammal's ability to detect and analyze spectral content in the environment, especially near threshold, at high acoustic frequencies (>10 kHz; *see* Ruggero and Santos-Sacchi (1997) for review). Damage to OHCs interferes with this process, and reduces system nonlinearities.

It is widely held that the active process involves voltage-driven mechanical responses of OHCs which provide feedback into the basilar membrane (Dallos, 1996). The molecular motors that reside in the lateral membrane of the OHC are bidirectional inasmuch as either membrane voltage or tension can evoke gating currents (Santos-Sacchi, 1991; Iwasa, 1993; Gale & Ashmore, 1994; Kakehata & Santos-Sacchi, 1995; Takahashi & Santos-Sacchi, 1998). Furthermore, the cell's voltage-dependent capacitance correlates well with its mechanical activity (Ashmore, 1989; Santos-Sacchi, 1990, 1991). It is expected, then, that nonlinear distortions that characterize the motility-related gating currents also describe concurrent mechanical responses. Indeed, harmonic mechanical responses and harmonic current responses have been observed in response to single sinusoidal stimulation of the OHC under whole cell voltage clamp (Santos-Sacchi, 1993).

Two-frequency evoked distortion components have been measured in the force of stereociliar bundles of Bullfrog saccular hair cells (Jaramillo, Markin & Hadspeth, 1993). From the bundle's resting position, AC stimulation produced distortion responses that were similar to those reported here. Sum and difference compo-

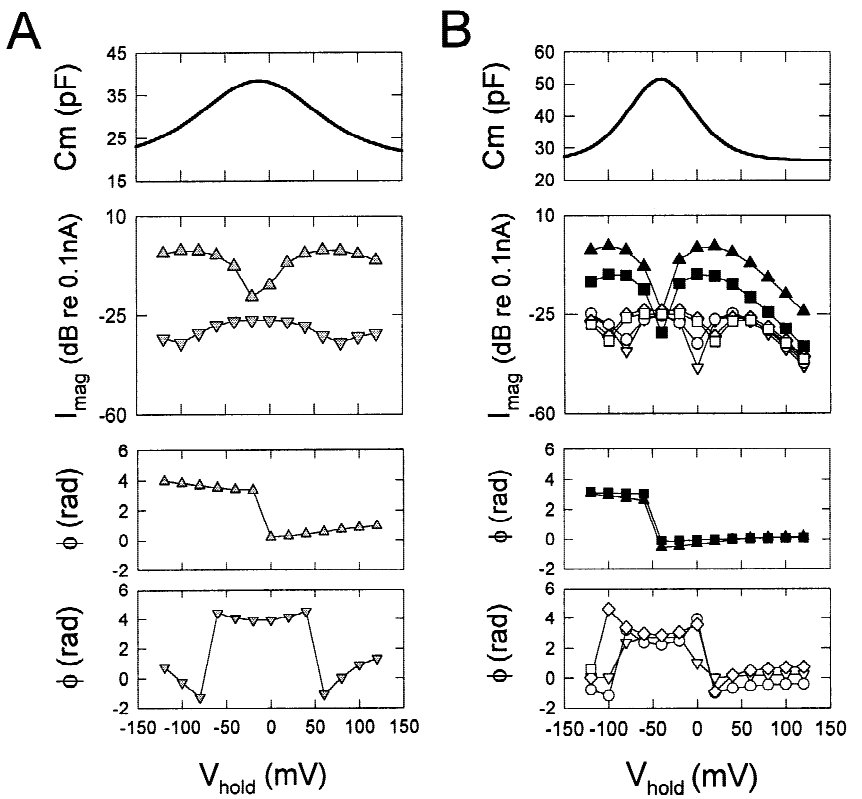

Fig. 8. Model simulation of OHCs under voltage clamp. The model consisted of an electrode resistance (R_s) in series with a parallel combination of membrane resistance (R_m) and capacitance (C_m), the capacitance being comprised of a linear (C_{lin}) and voltage-dependent component (C_v). The *panels A* and *B* correspond to those of Fig. 4, whose fitted cell parameters were used to generate the model distortion products shown here. Data were generated using the same stimulus protocols as in Fig. 4. In panel *A*, the membrane capacitance was modeled as in Eq. 1 with V_{pkcm}: −12.0 mV; *z*: 0.59; Q_{max}: 3.17 pC; and C_{lin}: 20.3 pF. R_s was 5 MΩ and R_m was 180 MΩ. In panel *B*, the membrane capacitance was modeled as in Eq. 1 with V_{pkcm}: −40.6 mV; *z*: 1.0; Q_{max}: 2.61 pC; and C_{lin}: 26.0 pF. R_s was 7 MΩ and R_m was 160 MΩ. The top panels illustrate the capacitance of each model cell, taken from Fig. 4 top panel fits. The symbols of the bottom panels show the generated distortion components as in Fig. 4. The lines simply connect the symbols. Note the similarities between model and biophysical data (Fig. 4).

nents were greatest in magnitude. It might be expected that in an analogous manner to the holding voltage manipulations reported here, stereocilia bundle biasing would produce magnitude and phase alterations in the force distortion components. Since the characteristics of OHC stereociliar bundles are basically the same as those of the lower vertebrate (Russell, Kossl & Richardson, 1992), it is expected that OHC stereocilia will likewise support distortion generation.

Despite the generation of distortion in single hair cells, significant differences exist between the characteristics of single cell distortion and distortion found in the intact auditory system. Indeed, while OHCs may ultimately underlie distortion found in the basilar membrane, inner hair cells and neural elements of the auditory system, it is unlikely that any single nonlinearity in a single hair cell can fully and simply account for the level and frequency-dependent behavior of distortion in the intact system. For example, in the basilar membrane, distortion levels decrease as the f2/f1 ratio is increased (Robles et al., 1997), but this ratio dependence is absent in isolated cells. One simple explanation for the in vivo dependence, alluded to by Robles et al. (1997) is the requirement for the two frequencies to reside within the excitation region of the cell. Thus, while delivery of disparate frequencies to single isolated cells is guaranteed experimentally, delivery to a single cell in vivo depends on the tuning characteristics of the basilar membrane. Only when frequencies are close enough to be within the excitatory bandwidth at a given stimulus level will an OHC receive two-tone stimulation. Another difference between system and cell is that distortion in vivo is robust at low stimulus levels. Nonlinearities in single cells are measured and predicted to decrease precipitously as stimulus levels decrease (Santos-Sacchi, 1993). This is shown here for the sum and difference distortion components (Fig. 5), where the rate of drop in magnitude is greater than that of the stimulating frequencies. Essentially, nonlinearities vanish at very small signal levels. In this regard, it should be stressed that the stereocilia transduction (displacement to receptor potential) function has a more significant nonlinearity near threshold than does the OHC motility function, indicating that the former is more likely to underlie the generation of nonlinearities in OHC mechanical responses that impinge on the basilar membrane (Santos-Sacchi, 1993). Thus, stereocilia may dominate distortion product generation whether or not stereocilia themselves are capable of mechanically influencing the cochlear partition. It is certainly conceivable, however, that alteration in the OHC motility nonlinearity may be observable in distortion components should the stereociliar nonlinearity remain stable. That is, modifications to the OHC lateral membrane motor alone will likely influence system nonlinearities.

Finally, a difference between single cell and basilar

membrane distortion that cannot be easily explained is the difference in the magnitude of distortion components. While the simple difference and sum components (f1+f2, f2−f1) were greatest in our single cell data, the stereociliar force production data (Jaramillo et al., 1993), and the OHC motility data (Hu et al., 1994), the greatest responses observed on the basilar membrane were the combination components, 2f2−f1 and 2f1−f2. Additionally, single cell distortion products were over an order of magnitude less than the stimulus frequency responses, while basilar membrane distortion could be greater — a result dependent upon tuning characteristics of the basilar membrane (Robles et al., 1997). Thus, it may be argued that the observed differences between intact system and single cell distortion call for an interaction of OHC assemblies to account for system nonlinearity characteristics. In line with this concept, we have recently shown that intact adjacent OHCs are mechanoelectrically coupled through supporting cells (Zhao & Santos-Sacchi, 1998). Furthermore, under dual voltage clamp, independent single sine wave stimulation in each cell generates combination distortion components in both cells (Zhao & Santos-Sacchi, 1999). In vivo, the extent of basilar membrane excitation distributions in the high frequency region of the cochlear can be taken to support interaction within OHC assemblies (Russell & Nilsen, 1997).

This work was supported by NIH-NIDCD grant DC00273 to JSS. We thank Margaret Mazzucco for technical help.

References

Ashmore, J.F. 1987. A fast motile response in guinea-pig outer hair cells: the cellular basis of the cochlear amplifier. *J. Physiol.* **388:**323–347

Ashmore, J.F. 1989. Transducer motor coupling in cochlear outer hair cells. *In:* Mechanics of Hearing. D. Kemp and J.P. Wilson, editors. pp. 107–113. Plenum Press, New York

Bezanilla, F., Taylor, R.E., Fernandez, J.M. 1982. Distribution and kinetics of membrane dielectric polarization. I. Long-term inactivation of gating currents. *J. Gen. Physiol.* **79:**21–40

Brownell, W.E., Bader, C.R., Bertrand, D., de Ribaupierre, Y. 1985. Evoked mechanical responses of isolated cochlear outer hair cells. *Science* **227:**194–196

Dallos, P. 1973. The Auditory Periphery: Biophysics and Physiology. Academic Press, New York

Dallos, P. 1996. Overview. *In:* P. Dallos, A.N. Popper and R.R. Fay, editors. pp. 1–43. The Cochlea, Springer, New York

Donnelly, D.F. 1994. A novel method for rapid measurement of Membrane Resistance, capacitance, and access resistance. *Biophys. J.* **66:**873–877

Fernandez, J.M., Bezanilla, F., Taylor, R.E. 1982. Distribution and kinetics of membrane dielectric polarization. II. Frequency domain studies of gating currents. *J. Gen. Physiol.* **79:**41–67

Fishman, H.M., Moore, L.E., Poussart, D. 1977. Asymmetry currents and admittance in squid axons. *Biophys. J.* **19:**177–183

Gale, J.E., Ashmore, J.F. 1994. Charge displacement induced by rapid stretch in the basolateral membrane of the guinea pig OHC. *Proc. Roy. Soc. Lond. B* **255:**243–249

Goldstein, J.L. 1967. Auditory nonlinearity. *J. Acoust. Soc. Am.* **41:**676–689

Goldstein, J.L., Kiang, N.Y.S. 1968. Neural correlates of the aural combination tone 2f1−f2. *Proc. IEEE* **56:**981–992

Hu, X.T., Evans, B.N., He, Z.Z., Dallos, P. 1994. Distortion products in electromotile responses of isolated outer hair cells. Abstracts of the Mid-winter Meeting of the Association for Research in Otolaryngology, St. Petersburg, FL, February

Huang, G., Santos-Sacchi, J. 1993. Mapping the distribution of the outer hair cell motility voltage sensor by electrical amputation. *Biophys. J.* **65:**2228–2236

Iwasa, K.H. 1993. Effect of stress on the membrane capacitance of the auditory outer hair cell. *Biophys. J.* **65:**492–498

Jaramillo, F., Markin, V.S., Hudspeth, A.J. 1993. Auditory illusions and the single hair cell. *Nature* **364:**527–529

Kakehata, S., Santos-Sacchi, J. 1995. Membrane tension directly shifts voltage dependence of outer hair cell motility and associated gating charge. *Biophys. J.* **68:**2190–2197

Kakehata, S., Santos-Sacchi, J. 1996. Effects of salicylate and lanthanides on outer hair cell motility and associated gating charge. *J. Neurosci.* **16:**4881–4889

Kim, D.O., Molnar, C.E., Matthews, J.E. 1980. Cochlear mechanics: nonlinear behavior in two-tone responses as reflected in cochlear-nerve-fiber responses and in ear canal sound pressure. *J. Acoust. Soc. Am.* **67:**1704–1721

Nuttall, A.L., Dolan, D.F. 1990. Inner hair cell responses to the 2f1−f2 intermodulation distortion product. *J. Acoust. Soc. Am.* **87:**782–790

Robles, L., Ruggero, M.A., Rich, N.C. 1991. Two-tone distortion in the basilar membrane of the cochlear. *Nature* **349:**413–414

Robles, L., Ruggero, M.A., Rich, N.C. 1997. Two-tone distortion on the basilar membrane of the chinchilla cochlear. *J. Neurophysiol.* **77:**2385–2399

Rohlicek, V., Rohlicek, J. 1993. Measurement of membrane capacitance and resistance of single cells using two frequencies. *Physiol. Res.* **42:**423–428

Ruggero, M.A. 1992. Responses to sound of the basilar membrane of the mammalian cochlea. *Neurobiology* **2:**449–456

Ruggero, M.A., Santos-Sacchi, J. 1997. Cochlear mechanics and biophysics. *In:* Handbook of Acoustics. M.J. Croker, Editor. John Wiley & Sons

Russell, I.J., Kossl, M., Richardson, G.P. 1992. Nonlinear mechanical responses of mouse cochlear hair bundles. *Proc. Roy. Soc.* **50:**217–227

Russell, I.J., Nilsen, K.E. 1997. The location of the cochlear amplifier: spatial representation of a single tone on the guinea pig basilar membrane. *Proc. Natl. Acad. Sci. USA* **94:**2660–2664

Santos-Sacchi, J., Dilger, J.P. 1988. Whole cell currents and mechanical responses of isolated outer hair cells. *Hearing Res.* **35:**143–150

Santos-Sacchi, J. 1990. Fast outer hair cell motility: how fast is fast? *In:* The Mechanics and Biophysics of Hearing. P. Dallos, C.D. Geisler, J.W. Matthews, M.A. Ruggero, and C.R. Steele, editors. pp. 69–75. Springer-Verlag, Berlin

Santos-Sacchi, J. 1991. Reversible inhibition of voltage dependent outer hair cell motility and capacitance. *J. Neurosci.* **11:**3096–3110

Santos-Sacchi, J. 1993. Harmonics of outer hair cell motility. *Biophys. J.* **65:**2217–2227

Santos-Sacchi, J., Kakehata, S., Takahashi, S. 1998. The outer hair cell membrane potential directly affects the voltage dependence of motility — related gating charge. *J. Physiol.* **510:**225–235

Takahashi, S., Santos-Sacchi, J. 1998. Tension-induced OHC gating currents are restricted to the cell's mid region. Abstracts of the Mid-winter Meeting of the Association for Research in Otolaryngology, St. Petersburg, FL, February

Takahashi, S., Santos-Sacchi, J. 1997. Distortion product analysis of outer hair cell motility-related gating currents. Abstracts of the Mid-winter Meeting of the Association for Research in Otolaryngology, St. Petersburg, FL, February

Takashima, S. 1978. Frequency domain analysis of asymmetry current in squid axon membrane. *Biophys. J.* **22:**115–119

Zhao, H.B., Santos-Sacchi, J. 1998. Mechano-electrical coupling among outer hair cells of Corti's organ. *Biophys. J.* **74:**A246 (*Abstr*.)

Zhao, H.B., Santos-Sacchi, J. 1999. Auditory collusion and a coupled couple of outer hair cells. *Nature* (*in press*)